The kinetic energy budget over North America during a period of major cyclone development

By PHILLIP J. SMITH,[1] *Advanced Study Program, National Center for Atmospheric Research,*[2] *Boulder, Colorado 80302, USA*

(Manuscript received February 8; revised version May 4, 1973)

ABSTRACT

The kinetic energy budget over North America is computed for a six day period spanning the pre-storm, growth, and decay stages of an intense cyclone. Regarding this region as comprising the total storm system, the results show that for the total system near balance between conversion of potential to kinetic energy and dissipation of kinetic energy occurs in the lower troposphere. However, in the upper troposphere the import of kinetic energy is an additional energy source which often exceeds the contribution from the conversion process. In addition the strong upper tropospheric flow is accompanied by a maximum in the dissipation. A composite energy budget for the immediate storm vicinity leads to conclusions which are qualitatively similar to those for the storm system, although the storm vicinity is energetically more intense than the total storm system by a factor of about three.

I. Introduction

Attention in the past two decades has focused on diagnoses of the energy sources, sinks, and transformations that are present as the atmosphere attempts to convert its supply of heat to motion (Oort, 1964; Starr & Saltzman, 1966; Lorenz, 1967). As a result it is now recognized that eddies assume the dominant role in the transfer and transformation of energy within the atmospheric general circulation. Even so, as pointed out by Johnson (1970), global analyses of eddy energy components often result in smoothing the contributions of individual systems which may have substantial rates of energy transformation but are relatively limited in their horizontal extent. Thus, a complete view of eddy processes requires an analysis of individual circulations systems.

Excepting the recent intense interest in tropical processes, much of the activity in meteorology has centered on the diagnosis and prognosis of middle latitude cyclones, anticyclones, and upper air waves and their attending weather events. Interest in the motions contained in such phenomena has motivated several studies of various aspects of their kinetic energy budgets; for example, Danard (1964), Eddy (1965), Palmén & Holopainen (1962), Sechrist & Rudy (1969), Sechrist & Dutton (1970), and Petterssen & Smebye (1971). These studies demonstrate that cyclones are complex systems capable of converting potential to kinetic energy, transferring energy from one scale to another, exporting or importing kinetic energy, and dissipating kinetic energy; and that in general all of these processes must be considered as important in the cyclone's life cycle.

The purpose of the present paper is to discuss the kinetic energy budget of North America during a period of major cyclone development, hoping to call further attention to the complex array of processes that must be accounted for in order to explain the behavior of these very important weather producing systems.

2. Computational aspects

A. *Basic equation.* The horizontal kinetic energy equation may be written as

[1] Permanent affiliation: Department of Geosciensciences, Purdue University, West Lafayette, Indiana 47907.

[2] The National Center for Atmospheric Research is sponsored by the National Science Foundation.

$$\int \frac{\partial k}{\partial t} = \int -\nabla \cdot k\mathbf{V} + \int -\frac{\partial \omega k}{\partial p} + \int -\mathbf{V} \cdot \nabla \phi + D \quad (1)$$
$$(a) \qquad (b) \qquad (c) \qquad (d) \quad (e)$$

where

$$\int = \frac{1}{gA} \iiint dx\, dy\, dp,$$

A = area of computational region,
∇ = horizontal del operator on a pressure surface,
$\mathbf{V}$ = horizontal wind vector with components (u,v)
ω = vertical motion in pressure coordinates (dp/dt),
k = $(u^2+v^2)/2$ = kinetic energy per unit mass,
ϕ = gz,
g = 980 cm sec^{-2},
z = geopotential height of pressure surfaces,
p = pressure,
x, y = west-east, south-north coordinates in a spherical, curvilinear coordinate system.

In spherical, curvilinear coordinates the del operation on a scalar (q) multiple of the vector wind is given by

$$\nabla \cdot q\mathbf{V} = \frac{\partial}{\partial x}(qu) + \frac{\partial}{\partial y}(qv) - qv \tan\theta / a \qquad (2)$$

where

a = radius of earth
θ = latitude.

Eq. (1) is the familiar Eulerian kinetic energy budget equation relating the time rate of change of kinetic energy (term 1a) over a computational region to a set of energy sources or sinks. Terms 1b and 1c are, respectively, the horizontal and vertical flux divergence (referred to in subsequent discussions as transports) of kinetic energy. Term 1d, labeled either kinetic energy generation (Kung, 1966) or conversion of potential to kinetic energy (Smith, 1970), reflects the production (or destruction) of kinetic energy by cross-isobaric flow. The final term is the very simple symbolic representation of a complex array of processes commonly identified as the dissipation of kinetic energy. As applied to computational studies over a finite data grid, dissipation contains two components: one, the viscous frictional loss of kinetic energy, and two, the transfer of kinetic energy either from or to sub-grid scale circulations through nonlinear interactions.

B. *Data used.* Estimates for the terms in (1) were obtained using standard 12 hr increment radiosonde wind and height data[1] for the stations depicted in Fig. 1 for the period 0000 GMT, 10 April through 0000 GMT, 16 April 1964. Computations were performed at the 64 stations located along and within the heavy black line with the remaining stations required for calculations at the lateral boundaries. Data were available in the vertical at the surface and in 50 mb increments from the first standard pressure level above the surface to 200 mb, the truncated upper boundary being dictated by the presence of unreliable wind observations above that level. The temporal and spatial resolutions of these data were sufficient to capture synoptic scale circulations before, during, and after development of a major tropospheric cyclone.

C. *Computing procedures.* All calculations were performed using unfiltered wind and height data. Although observational errors reside in these data, avoiding a filtering operation reduces the possibility of smoothing the more subtle spatial and temporal variations important in the evolving circulation features. Further, the author feels that averaging over a moderately large number of points yields mean quantities that are sufficiently accurate for meaningful diagnoses of kinetic energy budgets over regions encompassing middle latitude cyclone systems, particularly in view of the fact that prognostic equations are not involved, and, thus, spurious growth of errors with time is not of concern.

The first three terms on the right-hand side of (1) were calculated directly at each station, level, and observation time. The first-order derivatives required in 1b and 1d were estimated applying the two-dimensional, second-order Taylor's series model discussed by Chien & Smith (1973). The same technique was used to compute horizontal wind divergence, from which the vertical motion was estimated using the kinematic method and the adjustment procedure suggested by O'Brien (1970) and applied by Fankhauser (1969), Smith (1971), and Chien & Smith (1973). Boundary conditions were $\omega = 0$ at $p = 200$ mb and $\omega = u = v = 0$ at the surface. The author recognizes that the upper boundary

[1] Provided by National Climatic Center.

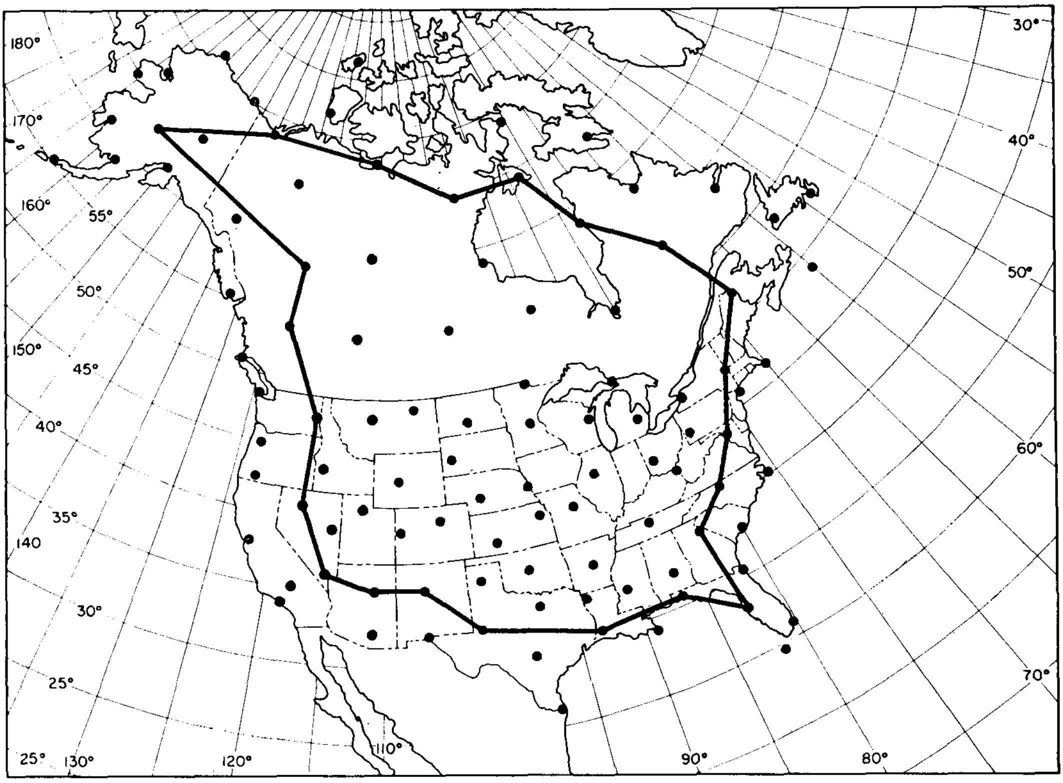

Fig. 1. Radiosonde stations utilized for budget computations (enclosed by heavy black line) and as additional boundary points.

condition limits stratospheric-tropospheric transport to those stations whose tropopause lies below 200 mb. While future studies utilizing more reliable higher level data ought not contain this restriction, the present calculations do at least implicitly contain consideration of such exchanges in the cold, postfrontal regions. Missing height data were linearly interpolated, while missing wind data were supplied according to the procedure of Chien & Smith.

The time derivative given by 1a was determined by simple finite difference over each time period and, therefore, represents the 12 hr time mean rate of change of kinetic energy. To provide comparable estimates, each of the right-hand quantities were averaged between succeeding 12 hr observational times. Vertical integrations were performed by the trapezoidal rule for the layers surface—800 mb, 800–600 mb, 600–400 mb, 400–200 mb, and for the entire surface—200 mb. Averages presented in subsequent tables were determined by simple average over the 64 station computational array. Calculations for individual twelve hour periods are presented for the entire surface to 200 mb layer. Results for individual layers are presented in the averages tabulated for the entire six day period.

D. *Dissipation term.* As is customary in large scale energy budget studies, the basic dissipation quantity was determined as the residual required to balance (1). Within the limitations of data errors, this procedure is adequate in the upper three layers. However, preliminary analyses of results in the lower boundary revealed unrealistically small values for terms 1d and 1e. The author has attributed these underestimates to the assumption of a zero wind at the earth's surface and insufficient vertical resolution near the ground which together result in failure to adequately account for surface drag. To obviate this difficulty the boundary layer dissipation model proposed by Lettau (1962) and applied to case studies by Bullock & Johnson (1971) and Gall & Johnson (1971) was used.

The applicable equation is

$$D = -\varrho c^2 v_g^3 \cos \alpha_0 \quad (3)$$

where

ϱ = density,
c = geostrophic drag coefficient,
v_g = geostrophic wind,
α_0 = angle between surface wind and isobars.

The drag coefficient is given by Kung's (1963) empirical relation

$$c = 0.205 \, [\log_{10}\{v_h(z_0 f)^{-1}\} - 0.556]^{-1} \quad (4)$$

where

z_0 = surface roughness parameter,
f = coriolis parameter.

Values assumed in the present calculations were $\varrho = 10^{-3}$ g cm^{-3}, $z_0 = 50$ cm, and $f = 10^{-4}$ sec^{-1}. Since the boundary layer problem was not recognized until after the calculations were completed, geostrophic winds were not available for this study. As a substitute for geostrophic winds, the area average surface—800 mb kinetic energy was used to obtain a root mean square wind speed for the lowest layer. The author recognizes that this procedure will tend to produce an underestimate of the mean dissipation because of failure to adequately account for the influence of strong wind areas. In order to partially compensate for this deficiency cos α_0 was maximized by setting $\alpha_0 = 0°$. This assumption also seems reasonable in view of the fact that observed rather than geostrophic winds were used. The results from calculations with (3) were used as dissipation estimates for the lowest layer. The energy conversion (term 1*d*) for the lowest layer was determined as the residual required to maintain balance.

3. Synoptic discussion

Surface, 500 mb, and 300 mb charts at 1200 GMT on each day are shown in Figs. 2–4, respectively. Surface charts depict isobars of sea level pressure in four millibar increments and surface fronts. Upper air charts contain contours of height with 60 meter increments at 500 mb and 120 meters at 300 mb. The 300 mb charts also include heavy arrows indicating maximum wind axes and dotted curves representing isotachs in knots. All charts are reproductions of standard National Meteorological Center analyses.

The data period began with high pressure dominant throughout most of the region. This anticyclonic influence persisted through 12 April, although weak cyclonic disturbances which failed to deepen appeared over south-central Canada and the Texas pahandle. The major cyclogenesis of particular interest in this study occurred at 1200 GMT, 12 April over eastern Colorado. The cyclone was characterized by slow deepening through its first 12 hours followed by rapid intensification to a central pressure of 972 mb by 1800 GMT, 13 April (Fig. 5). After reaching its peak intensity, the storm occluded and filled as it continued its northeastward movement across the north-central United States and Canada. Over the remaining North American continent, which in this case corresponds to the large scale interacting environment of the storm, the contrast between the cyclone's growth and decay and the following high pressure ridge invading across the Rocky Mountains produced strong pressure gradients and strong ageostrophic flow, particularly to the south and west of the cyclone.

Based on the surface charts and changes in central pressure, 0000 GMT, April 10–1200 GMT, April 12 will be referred to as the pre-storm period; 1200 GMT, April 12–0000 GMT, April 14 as the growth period; and the remaining as the decay period. Note that cyclogenesis occurred well within the data region and that the direction and speed of propagation of the storm allowed it to remain in the region for several days. Further, the dimensions of the cyclone were such that a diagnostic study over North America is equivalent to an analysis of the synoptic scale processes responsible for the storm's behavior.

The 500 mb flow was predominantly westerly and northwesterly through the pre-storm period, with only minor waves apparent. The 500 mb wave associated with the major cyclogenesis first appeared on 12 April over the Pacific northwest. This trough was characterized by weak diffluent flow ahead of the trough line

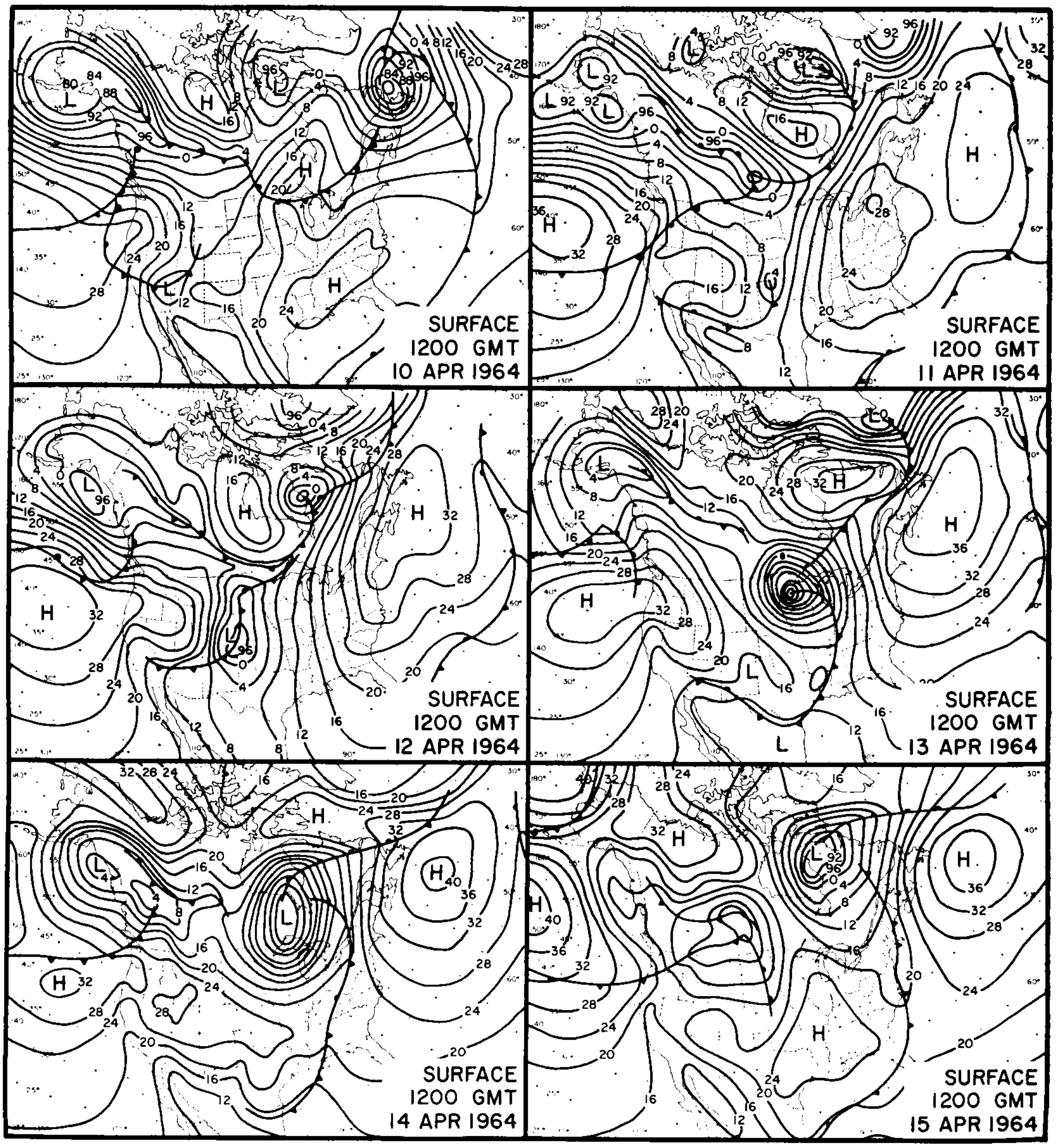

Fig. 2. Sea level isobars in millibars and surface fronts, 1200 GMT, 10–15 April 1964.

with strong northwesterly flow to the rear. The development of this diffluent wave can be explained by the strong vorticity advection into the trough region; or, as described by Krishnamurti (1968), by a transformation of shear vorticity into curvature vorticity. By 13 April a closed low appeared at 500 mb and the upper tropospheric mass divergence downstream from the wave no doubt contributed significantly to the deepening of the surface low pressure center. As the surface cyclone occluded, the 500 mb low assumed a position almost directly above the low level storm, a structure that persisted throughout the remaining decay period. The upper tropospheric circulation was marked by strong flow first to the west and then throughout the upper air wave. The prominence and persistence of the jet stream will later be seen to be significant in the energetics of the upper tropospheric flow.

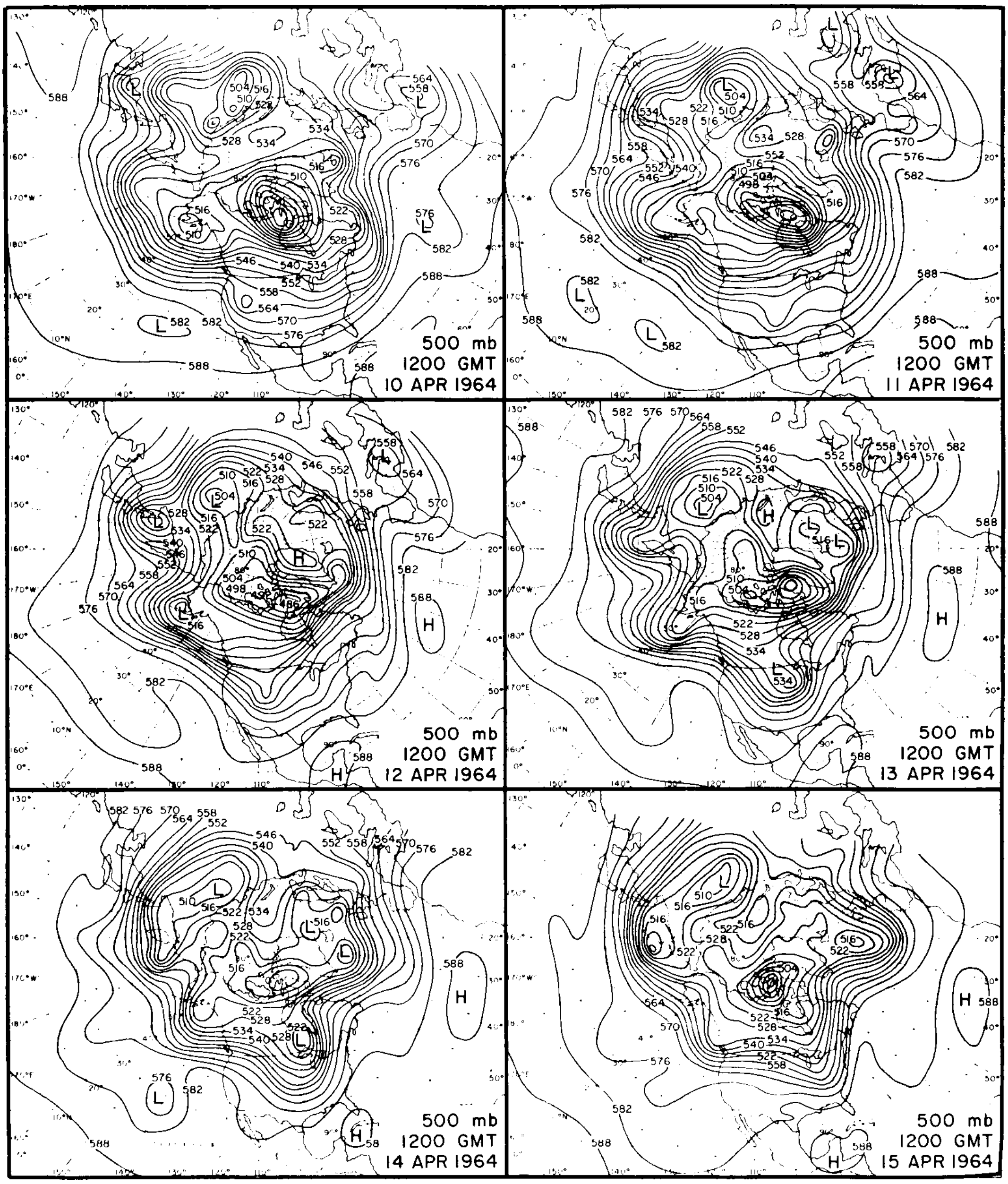

Fig. 3. 500 mb height contours in decameters, 1200 GMT, 10–15 April 1964.

4. Budget for storm system (North America)

Because of dominance of the low level cyclone, the preceding and following anticyclones, and the upper air waves over the data region, the energy budget calculations over North America will be considered to represent the energetics of the entire storm system. This is in contrast to later discussion of the energetics in the immediate storm vicinity. Table 1 contains the area average budget integrated from the surface to 200 mb for each 12 hr time period. Kinetic energy is given as 10^5 joules m^{-2}, while energy

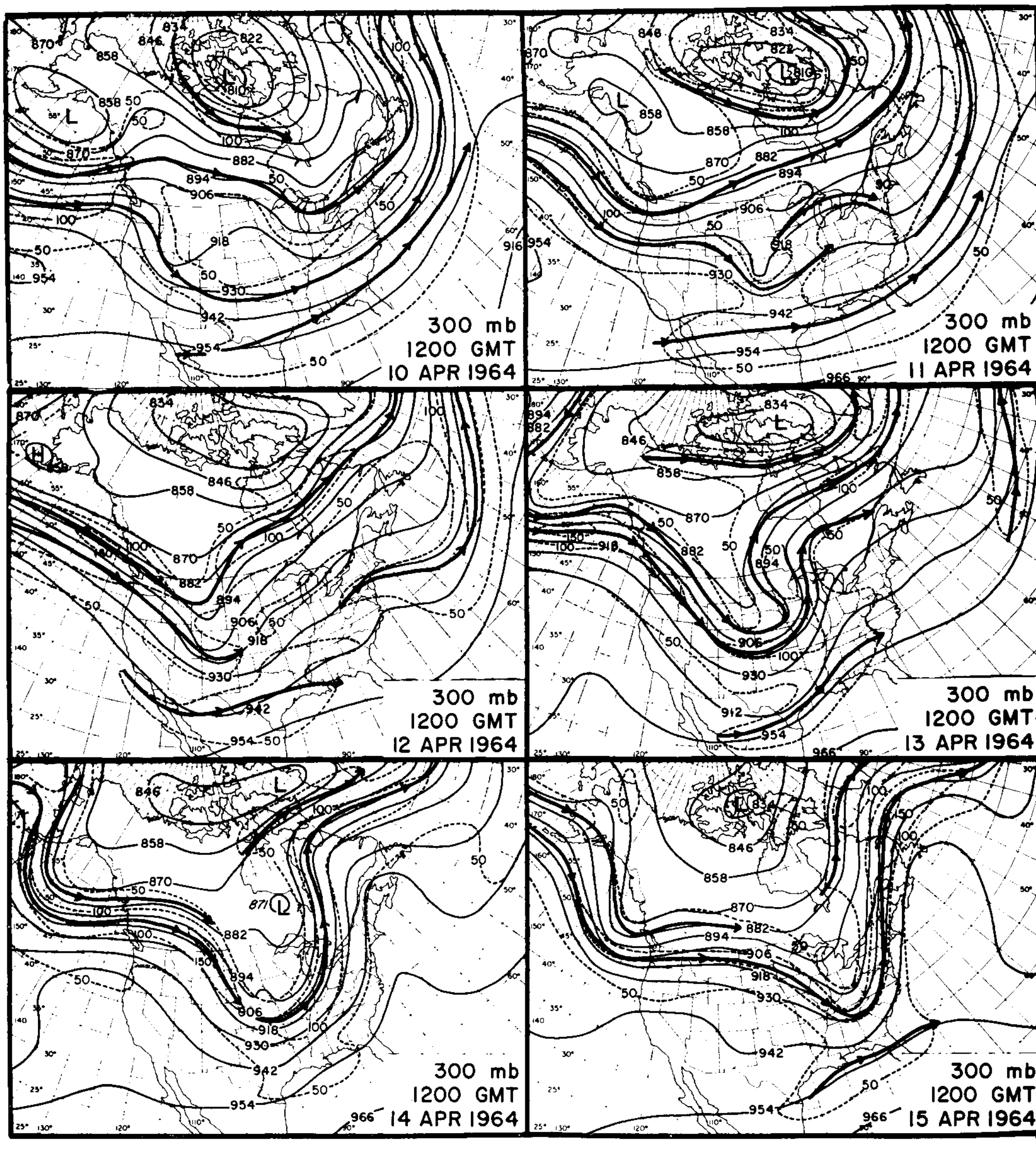

Fig. 4. 300 mb height contours in decameters (solid curves), maximum wind axes (heavy arrows), and isotachs in knots (dotted curves), 1200 GMT, 10–15 April 1964.

changes are in watts m^{-2}. In addition to the budget terms of (1), tabulations of $-\mathbf{V}\cdot\nabla\phi + D$ are included. The sum $-\mathbf{V}\cdot\nabla\phi + D$ represents the net *internal* source or sink of kinetic energy, which can be compared with the sum $-\nabla\cdot k\mathbf{V} - (\partial\omega k/\partial p)$, the *external* source or sink of kinetic energy. Note that for the surface -200 mb layer—$\partial\omega k/\partial p = 0$ and, therefore, is not presented in Table 1.

A. *Pre-storm period.* Through the total tropospheric layer (Table 1) kinetic energy decreases prevail prior to cyclogenesis. In the earlier periods these decreases are accompanied by negative or small values of horizontal transport, conversion of potential to kinetic energy, and dissipation. However, in the 12 to 24 hr period preceding cyclogenesis significant increases in the supply of kinetic energy from transport and

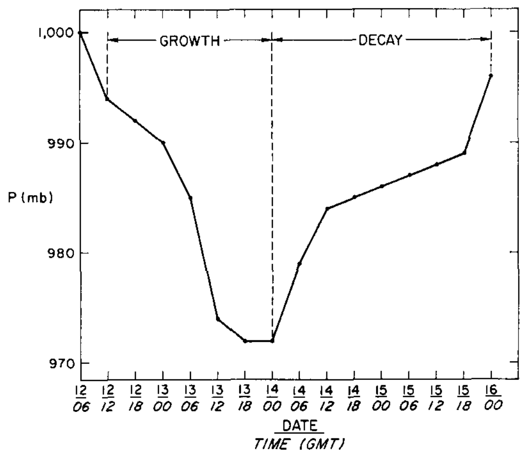

Fig. 5. Central pressure of major cyclone in millibars as a function of time in six hour increments.

energy conversion are observed. Balancing these energy sources are dramatic increases in energy dissipation. Alternately, the essentially zero change in kinetic energy during this 24 hr period may be thought of as resulting from near balance between the external source ($-\nabla \cdot k\mathbf{V}$) and internal sink ($-\mathbf{V}\cdot\nabla\phi + D$) of kinetic energy.

On 10 and 11 April, although maximum wind axes in the upper troposphere are plentiful, they reflect less intense winds than are prevalent on subsequent days. The flow exiting the region exceeds that entering; and, hence, the horizontal transport is negative. In the 12 to 18 hour period prior to cyclogenesis the intensity of flow across the western boundary has increased producing a marked increase in upper level kinetic energy import prior to cyclogenesis. The vorticity transport associated with this flow pattern provides a barotropic mechanism for deepening the diffluent trough invading western North America. As a result of this deepening, the enhanced gradients induce cross-isobaric flow and conversion of potential to kinetic energy. Both horizontal import and conversion are seen to be important sources of kinetic energy.

Of special interest are the dissipation estimates. Early in the pre-storm period positive dissipation values were obtained. In view of computational uncertainties, confidence in these estimates must necessarily be limited. However, it is likely that these values are at least small, and perhaps even positive, reflecting processes which increase the kinetic energy. If one accepts the notion that viscous dissipation must detract from the motions involved, then a positive value implies an enhancement of large scale kinetic energy due to the nonlinear cascade of energy from sub-grid to grid scale circulations. Unfortunately, since by definition such circula-

Table 1. *Kinetic energy budget for storm system (North America), surface to 200 mb*

Units: $k = 10^5$ joules m^{-2}, energy changes = watts m^{-2}, cg = cyclogenesis

Date/time	k	$\partial k/\partial t$	$-\nabla \cdot k\mathbf{V}$ (external)	$-\mathbf{V}\cdot\nabla\phi$	D	$-\mathbf{V}\cdot\nabla\phi + D$ (internal)	
Pre-storm							
10/00–10/12	16.2	0.2	−4.6	5.1	−0.3	4.8	
10/12–11/00	15.4	−3.7	−2.8	−1.9	1.0	−0.9	
11/00–11/12	14.2	−2.4	0.4	3.8	−6.6	−2.8	
11/12–12/00	13.5	−1.6	6.1	9.3	−17.0	−7.7	
12/00–12/12	13.4	2.1	10.8	12.1	−20.8	−8.7	
							cg
Growth							
12/12–13/00	15.7	8.6	13.9	4.8	−10.1	−5.3	
13/00–13/12	19.7	9.9	14.5	6.8	−11.4	−4.6	
13/12–14/00	23.6	0.6	7.4	18.4	−25.2	−6.8	
							peak
Decay							
14/00–14/12	21.8	−2.9	10.1	8.8	−21.8	−13.0	
14/12–15/00	19.6	−5.9	19.1	−5.9	−19.1	−25.0	
15/00–15/12	18.1	−1.0	9.1	−3.0	−7.1	−10.1	
15/12–16/00	16.8	−4.8	−0.4	0.3	−4.7	−4.4	

Table 2*A*. *Time mean kinetic energy budget for storm system*

0000 GMT, 10 April — 0000 GMT, 16 April 1964. Units same as Table 1

Layer	k	$\partial k/\partial t$	$-\nabla\cdot k\mathbf{V}$ (external)	$-\partial\omega k/\partial p$	$-\mathbf{V}\cdot\nabla\phi$	D	$-\mathbf{V}\cdot\nabla\phi+D$ (internal)
Surface–800 mb	1.1	0.0	0.0	−0.2	2.6	−2.4	0.2
800–600 mb	2.3	0.0	−0.2	0.1	1.0	−0.9	0.1
600–400 mb	5.0	0.0	0.7	0.5	0.3	−1.5	−1.2
400–200 mb	9.0	−0.1	6.4	−0.4	2.2	−8.3	−6.1
Surface–200 mb	17.4	−0.1	6.9	0.0	6.1	−13.1	−7.0

Table 2*B*. *Percentage contribution of each term to kinetic energy budget*

Layer	k	$\partial k/\partial t$	$-\nabla\cdot k\mathbf{V}$ (external)	$-\partial\omega k/\partial p$	$-\mathbf{V}\cdot\nabla\phi$	D	$-\mathbf{V}\cdot\nabla\phi+D$ (internal)
Surface–800 mb		00	00	04	50	46	
800–600 mb		00	09	05	45	41	
600–400 mb		00	23	17	10	50	
400–200 mb		01	37	02	13	47	
Surface–200 mb		00	27	00	23	50	

tions cannot be directly resolved in the computations, it is impossible to explicitly verify this conclusion. It is, however, interesting to note that during the two initial periods smaller grid scale waves exhibit a consistent tendency to damp out rather than grow. It seems plausible to the author that the stable flow may also be forcing sub-grid perturbations to damp out and thus contribute their energy to the larger scales. With the intrusion of major jet stream activity and increased flow over the mountainous west on 11 and 12 April production of turbulence and mountain waves penetrating into the upper troposphere will greatly increase the loss of large scale kinetic energy. Hence, the marked increases in horizontal transport and cross-isobaric flow are accompanied by increased dissipation.

B. *Growth period*. As the low level cyclone in the central United States and its associated upper air wave grew and increasingly dominated the circulations over North America, significant increases in kinetic energy occurred throughout the troposphere. On the whole, both horizontal import and conversion of potential to kinetic energy represent the sources of kinetic energy, while dissipation serves as the sink.

Although kinetic energy continues to be produced by the conversion term, the large dissipation values lead to a net internal sink of kinetic energy. Thus, in this case study horizontal import is necessary in order to maintain the observed kinetic energy increases. A curious feature of this period is the temporary decrease in the conversion from 1200 GMT, 12 April through 1200 GMT, 13 April, even though the wave patterns are undergoing rapid intensification. Realizing that to some extent computational uncertainty may be responsible, this may also be a result of the sizeable horizontal transports during and immediately preceding 13 April. Such transports are likely to produce super-geostrophic flow and motion toward higher height values at many data points. This in turn partially offsets the cross-contour flow toward lower height values that would be expected during wave deepening. As horizontal transport decreases toward the end of the period and the super-geostrophic flow attributed to it is reduced, conversion achieves its maximum value.

C. *Decay period*. The deterioration of the storm system is demonstrated by the steady decrease in its kinetic energy. This occurs despite the fact that horizontal transport continues to represent a major energy source. Though this provides a continued strong source of energy for the region it is in general located well west of the upper trough and is not able to provide a new energy source for the wave itself. In the absence of this support the wave diminishes, its conversion decreases and becomes negative, and the dissipation combines to yield an internal sink that exceeds the external source of kinetic energy.

D. *Time mean energy budget*. Table 2A presents for each layer the kinetic energy budget of the storm system averaged over all twelve

Table 3. *Composite kinetic energy budget for storm system by period*

Comparative results of Petterssen & Smebye (1971) and Sechrist & Rudy (1969). Units same as Table 1

Study	k	$\partial k/\partial t$	$-\nabla \cdot k\mathbf{V}$	$-\partial \omega k/\partial p$	$-\mathbf{V}\cdot\nabla\phi$	D	$-\mathbf{V}\cdot\nabla\phi + D$
Pre-storm period							
S (spring)							
Surface–200 mb	14.5	−1.1	2.3	0.0	5.8	−9.2	−3.4
P & S (winter)							
Surface–100 mg	27.8	−5.4	−13.1	−1.5	17.3	−8.1	9.2
Growth period							
S	19.2	6.5	12.0	0.0	10.0	−15.5	−5.5
S & R (spring)							
850–200 mb	19.0	2.6	1.6	0.0			1.0
P & S	27.0	2.8	−9.7	−1.0	19.8	−6.3	13.5
Decay period							
S	19.0	−3.6	9.5	0.0	0.1	−13.4	−13.1
P & S	26.3	−2.8	−9.4	−1.0	16.0	−8.4	7.6

time periods. Regarding these as the ensemble kinetic energy properties of the cyclone system, several interesting points emerge. First of all the kinetic energy approximately doubles through each successive layer. The factor of 8 change in k from the lower to upper layer and the corresponding threefold increase in mean wind speed reflect the persistence of the strong jet stream activity throughout the period. The most prominent results of these strong high level winds are the significant import of kinetic energy in the uppermost layer, a feature that is not present in the other three layers, and the very substantial dissipation induced by the turbulent energy exchange associated with these winds. In the lowest layer kinetic energy production is almost entirely a result of conversion of potential to kinetic energy. However, the energy gained in this manner is balanced by dissipation and vertical export of kinetic energy. Vertical transport is generally small; but when compared with other terms is a significant source of kinetic energy in middle layers. Finally, it is interesting to note that internal ($-\mathbf{V}\cdot\nabla\phi + D$) and external [$-\nabla\cdot k\mathbf{V} - (\partial\omega k/\partial p)$] contributions nearly balance in each layer.

An alternate way of analyzing the various budget quantities is to consider the relative contribution of each term. Table 2B contains the percentage contribution of the five primary budget quantities for each layer. Percentages were computed as the ratio of the absolute value of a quantity divided by the sum of absolute values of all five budget terms for a particular layer, all multiplied by 100. Clearly, the lower two layers are dominated by the conversion and dissipation processes. However, in the upper layers the relative importance of horizontal transport increases markedly, primarily at the expense of energy conversion. Dissipation maintains a nearly constant relative contribution throughout the troposphere. For the entire tropospheric layer horizontal transport and conversion represent nearly equal sources of kinetic energy and together resupply the kinetic energy dissipation in the region.

E. *Comparative results.* As is normally the case, it is of great interest to compare the results of a new study with those of other authors. In the present case comparison is made with the results of Petterssen & Smebye (1971), who computed the kinetic energy budget from the surface to 100 mb for a winter cyclone, and Sechrist & Rudy (1969), who computed a budget from 850 to 200 mb for a spring cyclone. Their results are summarized in Table 3 together with the average values from Table 1 for each storm period. For simplicity the author's results are indicated by S, Petterssen & Smebye by P & S, and Sechrist & Rudy by S & R. Note that S & R did not obtain separate estimates for $-\mathbf{V}\cdot\nabla\phi$ and D. Apologies are made for errors made by the author in interpolating values from graphs in the latter two papers.

The most consistent result among the three studies is the decrease in kinetic energy observed in the pre-storm and decay periods and the increase during storm growth. Beyond these statistics, however, there are very striking differences, in particular with regard to the roles of external versus internal terms. As previously noted, the present study demonstrates the impact of strong import of kinetic energy as a result of persistent jet stream intrusion into the region. This import is essential in this case to provide a net kinetic energy gain during the growth period and to slow the storm deterioration during the decay period. In each of the periods dissipation is sufficient to produce a net sink of kinetic energy in the internal term. The results of P & S are quite the opposite. In their case, which deepened to a central pressure similar to that of the present study, the major jet stream is exiting rather than entering the region, associated with a major cyclone over the Atlantic Ocean. Therefore, the transport is negative; and the conversion of potential to kinetic energy becomes the principal energy source for the storm system. With regard to dissipation, P & S note the relatively small wind shears present in their data which at least qualitatively accounts for their smaller dissipation estimates. The growth period results of S & R suggest a less dramatic case, a conclusion verified by the minimum central pressure of 990 mb. Examination of their 500 mb isotach analyses indicates that, while a significant jet stream is present within their region, persistent intrusion in the western boundary is not present. Thus, the horizontal flux is relatively small.

These comparisons call attention to two important considerations when interpreting Eulerian energy budget calculations. First, individual cases can differ greatly in their energetics and, therefore, presumably also in their dynamics. Second, the particular placement of the dominant circulation feature within the chosen data array can influence the mean budget calculations. In view of the small number of case studies done to date it would be most difficult to specify the "typical" energetic behavior of a middle latitude cyclone system.

5. Storm vicinity budget

While the preceding results are representative of the overall cyclone system, much insight can also be gained by examining the energetics in the immediate vicinity of the storm as it propagates through the data region. For this purpose stations were chosen that were located within the last closed isobar of standard surface analyses at the middle observation time within each twelve hour period. Sufficient definition of the storm was possible from the time of cyclogenesis (1200 GMT, 12 April) through 0000 GMT, 15 April, spanning the growth and early decay periods and including a total of 59 stations. The previously computed Eulerian budgets for each station were averaged to yield a composite Eulerian kinetic energy budget for the storm vicinity.

Results of these tabulations are presented in Table 4. Percentages in 4B were computed as in 2B. The surface—200 mb results once again show the very important role of horizontal transport which joins with energy conversion to nearly balance the energy loss due to dissipation. Also as seen in earlier statistics, there are significant differences between upper and lower layers. The lower troposphere shows a net internal production of kinetic energy with energy conversion and dissipation the dominant individual processes. In the upper troposphere transport represents a substantially greater kinetic energy source than does energy conversion and is of critical importance in compensating for the net internal loss of energy. The predominant upward motions in the storm vicinity yield a vertical exchange from the lowest three layers to the 400–200 mb layer. However, this is somewhat misleading, because the role of the downward motions west and southwest of the storm is not accounted for. Such subsiding motions will in general transport kinetic energy out of the upper troposphere to be realized as a kinetic energy source in the storm vicinity as it is horizontally transported in the lower troposphere. Such three-dimensional energy injection was suggested by Sechrist & Dutton (1970). Considered in the gross sense it is evident upon comparison with Table 2 that the storm vicinity is energetically more active than the total storm system by a factor of about three.

The energy conversion of 18.2 watts m^{-2} calculated in this study compares well with the values of 16 to 21 watts m^{-2} calculated by Väisänen (1961), Palmén & Holopainen (1962), and Danard (1964), as summarized by Palmén & Newton (1969). When compared with the 16.0 watts m^{-2} estimate of the generation of available potential energy in a storm of 1.1×10^3 km

Table 4A. *Composite storm vicinity budget*

1200 GMT, 12 April — 0000 GMT, 15 April. Units: watts m^{-2}

Layer	$\partial k/\partial t$	$-\nabla\cdot k\mathbf{V}$	$-\partial \omega k/\partial p$	$-\mathbf{V}\cdot\nabla\phi$	D	$-\mathbf{V}\cdot\phi+D$
Surface–800 mb	0.6	0.8	−0.7	8.9	−8.4	0.5
800–600 mb	2.1	0.7	−0.1	0.7	0.8	1.5
600–400 mb	1.9	4.9	−0.6	1.1	−3.5	−2.4
400–200 mb	−0.9	17.5	1.4	7.5	−27.3	−19.8
Surface–200 mb	3.7	23.9	0.0	18.2	−38.4	−20.2
Table 4B. *Percentage contribution of each term to kinetic energy budget*						
Surface–800 mb	3	4	4	46	43	
800–600 mb	48	16	2	16	18	
600–400 mb	16	41	5	9	29	
400–200 mb	2	32	2	14	50	
Surface–200 mb	4	28	0	22	46	

radius by Bullock & Johnson (1971), these conversion results suggest that much of the available potential energy produced within a significant extratropical cyclone is converted into kinetic energy within the storm itself. Finally, the boundary layer dissipation of −8.4 watts m^{-2} is comparable with the −7.5 watts m^{-2} obtained by Bullock & Johnson for the 1.1×10^3 km storm.

6. Conclusions

As expected, the mean kinetic energy budget in the boundary layer of both the storm system and storm vicinity is essentially an expression of balance between the baroclinic conversion of potential to kinetic energy ($-\mathbf{V}\cdot\nabla\phi$) and dissipation (D). However, the fact that exact balance is not achieved is quite important. First, the excess of conversion over dissipation in the lower layer is indicative of the intensification of the system in the region of the troposphere most responsible for observed weather changes. On the other hand, when dissipation exceeds conversion, storm decay is likely. Second, the small mean horizontal transport might conceal a barotropic energy source to the rear of the storm accomplished by three-dimensional import of kinetic energy originating in the upper troposphere upstream from the storm vicinity.

In the higher layers, where the dynamic mechanisms for reducing surface pressure often reside, the kinetic energy budget is much more responsive to energy transport. In the present case horizontal transport is a major energy source, equal to conversion in importance. In other cases it may be a sink; e.g., Petterssen & Smebye (1971). Further, in the presence of major jet stream activity and instability associated with deep cyclone development such as described in this paper, the dissipation of kinetic energy can reach sizeable levels. Dissipations obtained in this study reflect a steady progression from Kung's (1969) multi-annual mean of −4.3 watts m^{-2}, to the present −13.1 watts m^{-2} for a major cyclone system, and finally to −38.4 watts m^{-2} for the intense storm vicinity.

Clearly, extratropical cyclones and their attending wave systems represent very intense components of the atmospheric circulation that owe their behavior to a complex sequence of baroclinic and barotropic processes.

Acknowledgements

The author is indebted to Dr Chester Newton for his review of the original manuscript, to Miss Therese Malouf for typing the manuscript, and to Mr Lee Fortier for drafting the figures. This work was initiated at Purdue University under support by the Atmospheric Sciences Secion, National Science Foundation, Grant No. 10933 no. 1.

REFERENCES

Bullock, B. R. & Johnson, D. R. 1971. The generation of available potential energy by latent heat release in a mid-latitude cyclone. *Mon. Wea. Rev. 99*, 1–14.

Chien, H. & Smith, P. J. 1973. On the estimation of kinematic parameters in the atmosphere from radiosonde wind data. *Mon. Wea. Rev. 101*, 252–261.

Danard, M. B. 1964. On the influence of released latent heat on cyclone development. *J. Appl. Meteor. 3*, 27–37.

Eddy, A. 1965. Kinetic energy production in a mid-latitude storm. *J. Appl. Meteor. 4*, 569–575.

Fankhauser, J. C. 1969. Convective processes resolved by a mesoscale rawinsonde network. *J. Appl. Meteor. 8*, 778–798.

Gall, R. L. & Johnson, D. R. 1971. The generation of available potential energy by sensible heating: A case study. *Tellus 23*, 465–482.

Johnson, D. R. 1970. The available potential energy of storms. *J. Atmos. Sci. 27*, 727–741.

Krishnamurti, T. N. 1968. A study of a developing wave cyclone. *Mon. Wea. Rev. 96*, 208–217.

Kung, E. C. 1963. Climatology of aerodynamic roughness parameter in the planetary boundary layer over the northern hemisphere. Annual Report, Contract DR-36-039-AMC-00878, Department of Meteorology, University of Wisconsin, Madison.

Kung, E. C. 1966. Kinetic energy generation and dissipation in the large-scale atmospheric circulation. *Mon. Wea. Rev. 94*, 67–82.

Kung, E. C. 1969. Further study on the kinetic energy balance. *Mon. Wea. Rev. 97*, 373–381.

Lettau, H. H. 1962. Theoretical wind spirals in the boundary layer of a barotropic atmosphere. *Beitr. Phys. Atmos. 35*, 195–212.

Lorenz, E. N. 1967. *The nature and theory of the general circulation of the atmosphere.* WMO No. 218TP.115.161 pp.

O'Brien, J. J. 1970. Alternative solutions to the classical vertical velocity problem. *J. Appl. Meteor. 9*, 197–203.

Oort, A. H. 1964. On estimates of the atmospheric energy cycle. *Mon. Wea. Rev. 92*, 483–493.

Palmén, E. & Newton, C. W. 1969. *Atmospheric circulation systems.* Academic Press, New York, 603 pp.

Palmén, E. & Holopainen, E. O. 1962. Divergence, vertical motion and energy conversion between potential and kinetic energy in an extratropical disturbance. *Geophysica 8*, 89–113.

Petterssen, S. & Smebye, S. J. 1971. On the development of extratropical cyclones. *Quart. J. Roy. Meteor. Soc. 97*, 457–482.

Sechrist, F. S. & Dutton, J. A. 1970. Energy conversions in a developing cyclone. *Mon. Wea. Rev. 98*, 354–362.

Sechrist, F. S. & Rudy, R. A. 1969. Kinetic energy changes in a developing cyclone. Final Report, ESSA Grant WBG 52, Department of Meteorology, University of Wisconsin, Madison.

Smith, P. J. 1970. A note on energy conversions in open atmospheric systems. *J. Atmos. Sci. 27*, 518–521.

Smith, P. J. 1971. An analysis of kinematic vertical motions. *Mon. Wea. Rev. 99*, 715–724.

Starr, V. P. & Saltzmann, B. 1966. Observational studies of the atmospheric general circulation. Scientific Report No. 2, Planetary Circulations Project, Massachusetts Institute of Technology, V. P. Starr, Director, 700 pp.

Väisänen, A. 1961. Investigations of the vertical air movement and related phenomena in selected synoptic situations. *Soc. Sci. Fennica, Commentationes Phys.-Math. 26*, 1–72.

БЮДЖЕТ КИНЕТИЧЕСКОЙ ЭНЕРГИИ НАД СЕВЕРНОЙ АМЕРИКОЙ В ПЕРИОД СИЛЬНОГО ЦИКЛОНИЧЕСКОГО РАЗВИТИЯ

Вычисляется бюджет кинетической энергии над Северной Америкой за период в шесть дней, охватывающий предварительную стадию, рост и затухание интенсивного циклона. Если рассматривать эту область как полностью охватывающую циклоническую систему, то результаты показывают, что в нижней тропосфере состояние близко к балансу между конверсией потенциальной энергии в кинетическую и диссипацией кинетической энергии. Однако в верхней тропосфере импорт кинетической энергии является дополнительным энергетическим источником, вклад которого часто превосходит вклад от конверсии. К тому же интенсивное течение в верхней тропосфере сопровождается максимумом диссипации. Полный бюджет энергии для непосредственной окрестности циклона качественно согласуется с бюджетом всей циклонической системы, хотя первый примерно в три раза энергетически более интенсивен.